

Transport control in deterministic ratchet system

Woo-Sik Son,^{1,2,*} Jung-Wan Ryu,³ Dong-Uk Hwang,⁴ Soo-Young Lee,² Young-Jai Park,^{1,†} and Chil-Min Kim^{2,‡}

¹*Department of Physics, Sogang University, Seoul 121-742, Korea*

²*National Creative Research Initiative Center for Controlling Optical Chaos, Pai-Chai University, Daejeon 302-735, Korea*

³*Department of Physics, Pusan National University, Busan 609-735, Korea*

⁴*Department of Biomedical Engineering, University of Florida, Florida 32611-6131*

(Dated: August 13, 2018)

We study the control of transport properties in a deterministic inertia ratchet system via the extended delay feedback method. A chaotic current of a deterministic inertia ratchet system is controlled to a regular current by stabilizing unstable periodic orbits embedded in a chaotic attractor of the unperturbed system. By selecting an unstable periodic orbit, which has a desired transport property, and stabilizing it via the extended delay feedback method, we can control transport properties of the deterministic inertia ratchet system. Also, we show that the extended delay feedback method can be utilized for separation of particles in the deterministic inertia ratchet system as a particle's initial condition varies.

PACS numbers: 05.40.-a, 05.45.Gg, 05.45.Pq, 05.60.Cd

I. INTRODUCTION

The ratchet effect, i.e., a directional motion of a particle using unbiased fluctuations, has attracted much attention in recent years [1, 2]. An early motivation in this field is to explain an underlying mechanism of molecular motors which transport molecules in the absence of appropriate potential and thermal gradients [3]. Lately, the ratchet effect has been studied theoretically and experimentally in many different fields of science, e.g., asymmetric superconducting quantum interference devices [4], quantum Brownian motion [5], Josephson-junction arrays [6], application for separation of particles [7], etc. It has been known that two conditions should be met to obtain the ratchet effect [1]. First, a system has to be in a non-equilibrium state by a correlated stochastic [8] or a deterministic perturbation [9]. Second, the breaking of the spatial inversion symmetry is required. In doing so, an asymmetric periodic potential, named the “ratchet potential”, is introduced.

Recently, several works concerning the control of ratchet dynamics have been presented. The applying of a weak subharmonic driving in a deterministic inertia ratchet system was used to enlarge the parameter ranges where regular currents are observed [10], and the signal mixing of two driving forces was considered to control transport properties in a overdamped ratchet system [11]. Also, the effect of time-delayed feedback on the ratchet system has been studied. The anticipated synchronization was observed in delay coupled inertia ratchet systems [12] and the stabilization of chaotic current to low-period orbits was presented, using time-delayed feedback methods, in the deterministic inertia ratchet system [13].

Starting with the work of Ott, Grebogi, and Yorke [14], various methods for controlling chaotic dynamics have been developed [15]. Particularly, Pyragas proposed a simple and efficient method, which utilizes a control signal with a difference between the present state of the system and the previous state delayed by the period of an unstable periodic orbit (UPO) [16]. This method is non-invasive in the sense that the control signal vanishes when the targeted UPO embedded in a chaotic attractor is stabilized. Some limitations on the Pyragas method have been reported [17] and the modifications of the Pyragas method have been proposed to improve its efficiency [18, 19]. Socolar *et al.* presented a method utilizing information from many previous states of the system, and this method is called the *extended time-delay autosynchronization* or the *extended delay feedback* (EDF) [18]. The stability and analytical properties of a delayed feedback system have been investigated [20].

In this paper, we aim to control transport properties of the deterministic inertia ratchet system. For this purpose, we have controlled a chaotic current of the system to a regular current by stabilizing an unstable periodic orbit which has a desired mean velocity, via the EDF method. Also, we have shown that the EDF method can be utilized for separation of particles in the deterministic inertia ratchet system as a particle's initial condition varies. The rest of the paper is organized as follows. In Sec. II, we have shown transport properties of the unperturbed deterministic inertia ratchet system. In Sec. III, the system controlled via the EDF method has been presented and the linear stability analysis of a periodic orbit in the presence of the EDF has been considered. In Sec. IV, via the EDF method, we have shown achievements of the desired transport properties of the system and a separation of particles has also been presented as varying particle's initial condition. The paper finishes with conclusions in Sec. V.

*Electronic address: dawnmail@sogang.ac.kr

†Electronic address: yjpark@sogang.ac.kr

‡Electronic address: chmkim@mail.pcu.ac.kr

II. DETERMINISTIC RATCHET SYSTEM

The deterministic inertia ratchet system is written as the following dimensionless equation,

$$\ddot{x} + b\dot{x} + V'(x) = a \cos(\omega_0 t). \quad (1)$$

Here, $V'(x)$ denotes the derivative with respect to x and b is the friction coefficient. ω_0 and a are the frequency and amplitude of the driving force, respectively. Figure 1 shows an asymmetric periodic potential, i.e., the ratchet potential $V(x)$ described by

$$V(x) = C - \left(\sin(2\pi(x-d)) + \frac{1}{4} \sin(4\pi(x-d)) \right) / 4\pi^2 \delta, \quad (2)$$

where d , δ and C are introduced so that the ratchet potential has a minimum at $x = 0$ with $V(0) = 0$.

This system exhibits both regular and chaotic behaviors, depending on parameters (a, b, ω_0) [21, 22, 23]. In this paper, we vary only the parameter a , and set $b = 0.1$ and $\omega_0 = 0.67$. General transport properties of the deterministic inertia ratchet system are shown in Fig. 2. In Fig. 2(a), we plot a bifurcation diagram of the stroboscopic recording of a particle's velocity at $t = kT$, where k is a positive integer and T is the period of the driving force. The mean velocity of the system as a function of the parameter a is depicted in Fig. 2(b). As shown in Fig. 2(b), multiple current reversals occur as the amplitude of the driving force is varied. It has also been observed that the current reversal is related to a bifurcation from chaotic to regular regime [21] and that the type-I intermittency exists in this bifurcation [22].

When the system exhibits a regular behavior, the time required for a particle to move from one well of the potential to another is commensurable with the period of the driving force. Hence, the mean velocity of a regular current shows a locking phenomenon given as follows:

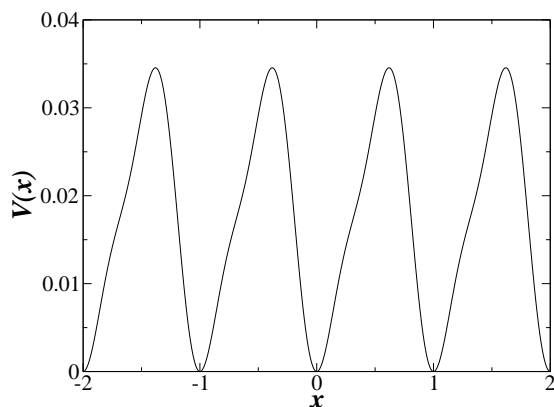


FIG. 1: Asymmetric periodic potential, i.e., the ratchet potential $V(x) = C - (\sin(2\pi(x-d)) + \frac{1}{4} \sin(4\pi(x-d))) / 4\pi^2 \delta$ with $d = -0.19$, $\delta = (\sin(2\pi|d|) + \sin(4\pi|d|)) / 4\pi^2$, and $C = -(\sin(2\pi d) + 0.25 \sin(4\pi d)) / 4\pi^2 \delta$.

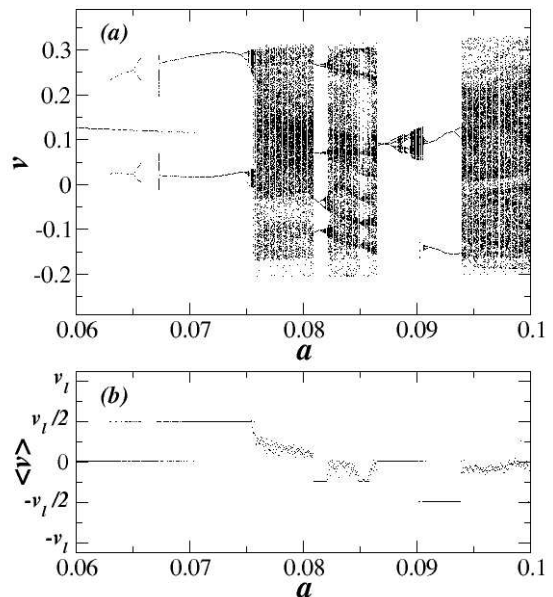


FIG. 2: Bifurcation diagrams as a function of a at $b = 0.1$ and $\omega_0 = 0.67$. In the region from $a = 0.063$ to 0.071 , coexisting attractors are found; (a) the stroboscopic recording of particle velocity, (b) the mean velocity of current.

$$\langle v \rangle = \frac{n L}{m T} = \frac{n \omega_0}{m 2\pi} L = \frac{n}{m} v_l, \quad (3)$$

where L is the spatial period of the ratchet potential ($L = 1$, as shown in Fig. 1, then $v_l = \frac{\omega_0}{2\pi}$), T is the time period of the driving force, and $\frac{n}{m}$ is an irreducible fraction ($n, m \in \mathbb{Z}$) [23]. v_l is the fundamental locking velocity corresponding to a particle's current which advances one well of the ratchet potential in a positive direction with the period of the driving force. As shown in Fig. 2, the system exhibits regular behaviors in some parameter ranges; a period-1 orbit with $\langle v \rangle = 0$ ($a = 0.06$), a period-2 orbit with $\langle v \rangle = \frac{1}{2} v_l$ ($a = 0.074$), a period-4 orbit with $\langle v \rangle = -\frac{1}{4} v_l$ ($a = 0.081$), and a period-2 orbit with $\langle v \rangle = -\frac{1}{2} v_l$ ($a = 0.092$). When the system shows a chaotic behavior, the mean velocity of the chaotic current is almost zero averaged.

It is worthy of note that there are various UPOs embedded in a chaotic attractor of the unperturbed system and that their mean velocities agree with Eq. (3). By stabilizing an UPO that has a desired mean velocity (i.e., written by specific n and m in Eq. (3)), we can achieve a desired regular transport of the deterministic inertia ratchet system instead of the zero averaged chaotic current. In this system, the periodic orbit is defined by $(\tilde{x}(t), v(t)) = (\tilde{x}(t+\tau), v(t+\tau))$, where $\tilde{x}(t) = x(t) \pmod{1}$ and τ is the time period of the orbit. We are interested in stabilizing some targeted UPOs among various UPOs that agree with Eq. (3). In Fig. 3, we have shown several UPOs, which are desired to be stabilized, located

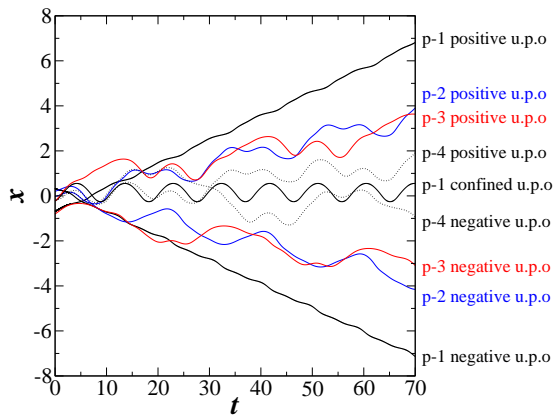


FIG. 3: (Color online) Unstable periodic orbits. period-1 (black line), period-2 (blue line), period-3 (red line), and period-4 orbits (dotted black line) obtained from the unperturbed system at $a = 0.083$.

by the Newton method. For period- n orbits, we consider two UPOs that have the same period $\tau = nT = 2n\pi/\omega_0$ with different mean velocities, where $n = 1, 2, 3, 4$: one is a positive current with the mean velocity $\langle v \rangle = \frac{1}{n}v_l$ and the other is a negative current with the mean velocity $\langle v \rangle = -\frac{1}{n}v_l$. Particularly, period-1 orbits include an oscillating orbit confined in one well of the potential with the mean velocity $\langle v \rangle = 0$. By selecting a specific UPO and stabilizing it via the EDF method, we can easily control transport properties of the deterministic inertia ratchet system.

III. LINEAR STABILITY ANALYSIS OF PERIODIC ORBITS

The deterministic inertia ratchet system controlled by the EDF method is described as

$$\ddot{x} + b\dot{x} + V'(x) = a \cos(\omega_0 t) + F, \quad (4)$$

where F is a control signal, i.e., the delayed feedback described by the particle's present velocity and the previous velocities delayed by multiples of the period of UPO. F is denoted by

$$F = K((1 - R) \sum_{m=1}^{\infty} R^{m-1} \dot{x}(t - m\tau) - \dot{x}(t)), \quad (5)$$

where K is a strength of feedback, τ is a delay time, which coincides with the period of the targeted UPO, and R ($0 \leq R < 1$) is a parameter that adjusts the distribution of each term's magnitude in the control signal. When $R = 0$, the EDF method is the same as the Pyragas method, i.e., $F = K(\dot{x}(t - \tau) - \dot{x}(t))$.

Now, let us consider the linear stability analysis of a periodic orbit in the presence of the EDF. Let the small

deviation from the periodic orbit $\xi_0(t)$ be $\delta\xi(t) = \xi(t) - \xi_0(t)$. According to the Floquet theory, $\delta\xi(t)$ can be described as

$$\delta\xi(t) = \sum_{k=1}^N C^{(k)} e^{(\lambda_k + i\omega_k)t} \mathbf{u}_k(t), \quad (6)$$

where $\lambda_k + i\omega_k$ is the Floquet exponent and $\mathbf{u}_k(t) = \mathbf{u}_k(t + \tau)$ is an eigenvector. $C^{(k)}$ is a constant and N is the dimension of the Poincaré surface. For one such mode, one can obtain the following deviation relation (dropping the index k). After the period τ of the periodic orbit has passed, the deviation is described as

$$\begin{aligned} \delta\xi(t + \tau) &= \exp((\lambda + i\omega)(t + \tau)) \mathbf{u}(t + \tau) \\ &= \exp((\lambda + i\omega)\tau) \delta\xi(t) \equiv (\Lambda + i\Omega) \delta\xi(t), \end{aligned} \quad (7)$$

where $\Lambda + i\Omega$ is the Floquet multiplier. When the delay terms are included, the phase space of the system becomes infinite dimensional and the system has an infinite number of Floquet multipliers. If the largest Floquet multiplier satisfies $|\Lambda_1 + i\Omega_1| < 1$, i.e., the leading Floquet exponent λ_1 ($\lambda_1 = \ln |\Lambda_1 + i\Omega_1|/\tau$) is less than zero, thereby the targeted UPO is stabilized.

The time evolution of $\delta\xi(t)$ is given by

$$\begin{aligned} \delta\dot{\xi} &= \begin{pmatrix} 0 & 1 \\ -V''(x) & -b \end{pmatrix} \delta\xi(t) \\ &+ \begin{pmatrix} 0 & 0 \\ 0 & 1 \end{pmatrix} K((1 - R) \sum_{m=1}^{\infty} R^{m-1} \delta\xi(t - m\tau) - \delta\xi(t)), \end{aligned} \quad (8)$$

where the matrix in the first term in Eq. (8) is the Jacobian of the unperturbed system and the second term comes from the presence of the EDF. The delayed terms in Eq. (8) can be eliminated and consequently the time evolution of the small deviation from the periodic orbit could be governed by

$$\delta\dot{\xi} = \begin{pmatrix} 0 & 1 \\ -V''(x) & -b - K \frac{1 - \frac{1}{\Lambda + i\Omega}}{1 - \frac{R}{\Lambda + i\Omega}} \end{pmatrix} \delta\xi(t) = A \delta\xi(t), \quad (9)$$

where the ratio of geometric series has a constraint $\frac{R}{|\Lambda + i\Omega|} < 1$ for convergence. For an elimination of the delay terms, we use the relation

$$\delta\xi(t - n\tau) = (\Lambda + i\Omega)^{-n} \delta\xi(t), \quad (n = 1, 2, 3, \dots). \quad (10)$$

Eq. (9) requires information of the targeted UPO. Hence, the Floquet multiplier is related to the eigenvalue problem of the monodromy matrix Φ_τ , which satisfies

$$\dot{\Phi}_t = A\Phi_t, \quad \Phi_0 = I. \quad (11)$$

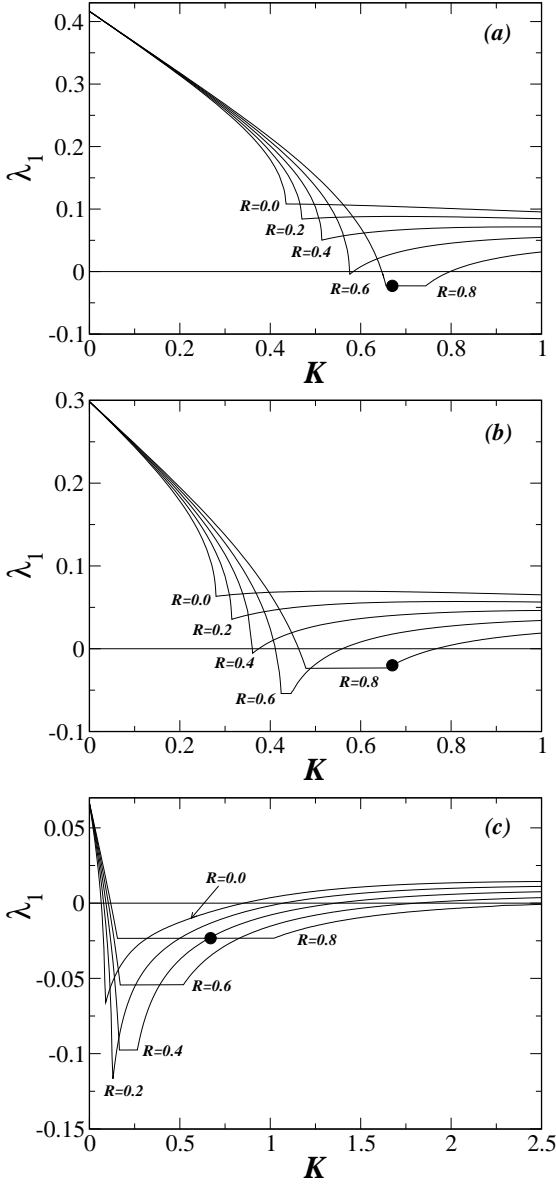


FIG. 4: The leading Floquet exponents of period-1 orbits; (a), (b), and (c) exhibit the leading Floquet exponents for the positive, the negative, and the confined currents as a function of K for the given R , respectively.

The eigenvalue of Φ_τ defines the Floquet multiplier as follows:

$$\det[\Phi_\tau - (\Lambda + i\Omega)I] = 0. \quad (12)$$

The Floquet multipliers are obtained by numerically solving Eqs. (9),(11), and (12). The results of leading Floquet exponents are shown in Figs. 4, 5, 6, and 7 for period-1 ($\tau = T = 2\pi/\omega_0$), period-2 ($\tau = 2T$), period-3 ($\tau = 3T$), and period-4 orbits ($\tau = 4T$), respectively. Each figure shows the leading Floquet exponent λ_1 as a function of the strength of feedback K for different values of the control parameter R . The results tell us

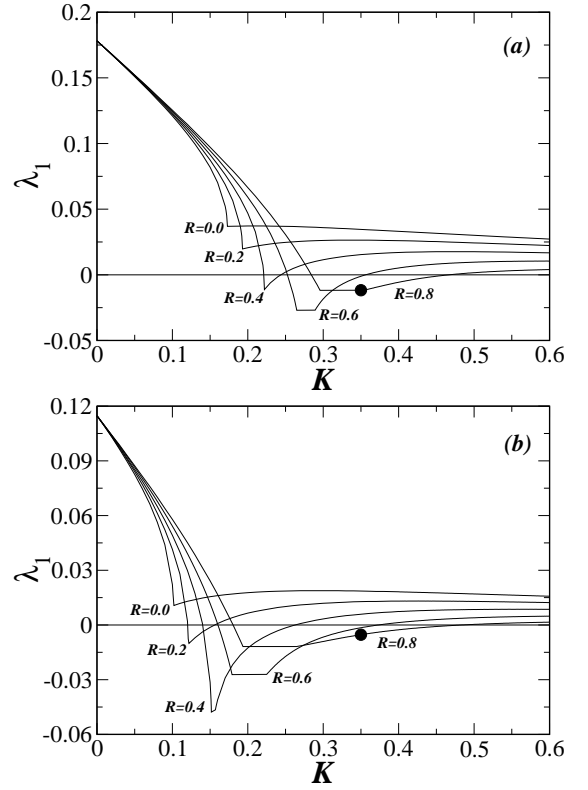


FIG. 5: The leading Floquet exponents of period-2 orbits; (a) and (b) exhibit the leading Floquet exponents for the positive and the negative currents as a function of K for the given R , respectively.

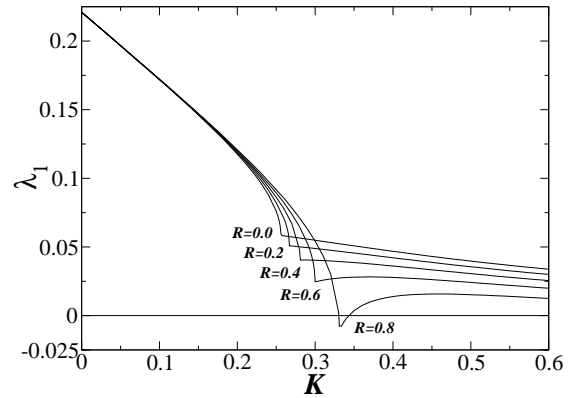


FIG. 6: The leading Floquet exponent of the period-3 positive orbit as a function of K for the given R .

the stabilized region of control parameters (K, R, τ) , in which the targeted UPO is stabilized ($\lambda_1 < 0$).

As shown in Fig. 4, the period-1 positive and the negative currents cannot be stabilized by the Pyragas method ($R = 0$). The positive current is stabilized at $R \geq 0.6$, the negative current is stabilized at $R \geq 0.4$, and the confined current, which only exists for the case of the period-1 orbits, can be stabilized even at $R = 0$. Such a phenomenon is roughly explained by the different degrees

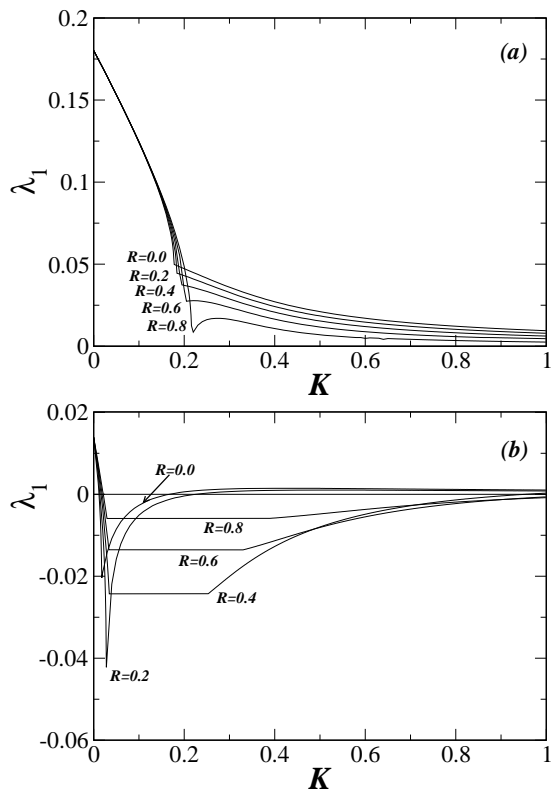


FIG. 7: The leading Floquet exponents of period-4 orbits; (a) and (b) exhibit the leading Floquet exponents for the positive and the negative currents as a function of K for the given R , respectively.

of instability of UPOs in the unperturbed system (see λ_1 values at $K = 0$ in Fig. 4). With the larger degree of instability in the unperturbed system, the UPO can be stabilized with a larger R . The stabilized region of K for the given R increases as R increases and if R is not very large, then the minimum of λ_1 is deeper as R increases. The EDF method ($0 < R < 1$) is more effective than the Pyragas method ($R = 0$).

Another interesting property of the EDF method is a limitation on the minimum of λ_1 for given control parameters R and τ . As shown in Fig. 4, the leading Floquet exponent is always larger than λ^* , where $\lambda^* = \ln(R)/\tau$. λ^* is given by the constraint on the ratio of geometric series. In Eqs. (8)-(10), the system gains the limit of geometric summation of the delayed feedback terms, which do not diverge, when the Floquet exponent is infinitesimally larger than λ^* . λ^* of the period-1 orbits ($\tau = T = 2\pi/\omega_0$) is numerated as $\lambda^* \simeq -0.1716$ ($R = 0.2$), -0.0977 ($R = 0.4$), -0.0544 ($R = 0.6$), and -0.0237 ($R = 0.8$). If the result of the Floquet exponent obtained by solving Eqs. (9), (11), and (12) is far from λ^* for given R and τ , then the shape of $\lambda_1(K)$ makes a narrow valley. If the result is very close to λ^* , then the shape of $\lambda_1(K)$ makes a valley with a flat bottom. In this case, the minimum of λ_1 is infinitesimally larger than λ^* and λ_1 is very slowly increasing as K increases.

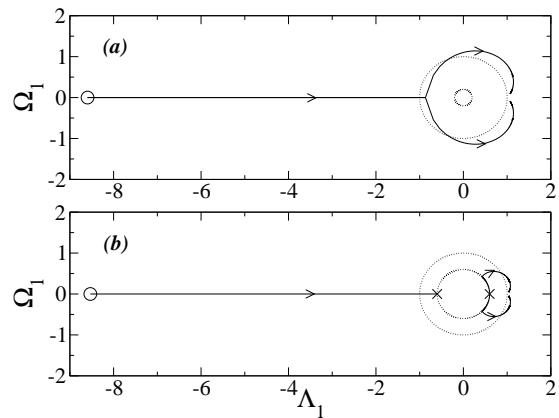


FIG. 8: The loci of the largest Floquet multiplier of period-2 negative orbit as K varies from 0 to ∞ ; (a) loci at $R = 0.2$ and (b) loci at $R = 0.6$. The outer (inner) circle has a radius of 1 (R). The open circle and the crosses denote the location of the largest Floquet multiplier at $K = 0$ and the discontinuity, respectively. For $K \rightarrow \infty$, the largest Floquet multiplier approaches $(\Lambda_1, \Omega_1) = (1, 0)$ in both cases of (a) and (b).

The leading Floquet exponents for period-2, period-3, and period-4 orbits are shown in Figs. 5, 6, and 7, respectively. The results are qualitatively equivalent to those of period-1 orbits shown in Fig. 4. The period-2 positive current is stabilized at $R \geq 0.4$, and the period-2 negative current is stabilized at $R \geq 0.2$. λ^* of the period-2 orbits ($\tau = 2T = 4\pi/\omega_0$) is numerated as $\lambda^* \simeq -0.0858$ ($R = 0.2$), -0.0488 ($R = 0.4$), -0.0272 ($R = 0.6$), and -0.0118 ($R = 0.8$). The period-3 negative current is stabilized at $R \geq 0.8$. λ^* of the period-3 orbit ($\tau = 3T = 6\pi/\omega_0$) is numerated as $\lambda^* \simeq -0.0572$ ($R = 0.2$), -0.0325 ($R = 0.4$), -0.0181 ($R = 0.6$), and -0.0079 ($R = 0.8$). The period-3 positive current cannot be stabilized by the EDF method because the largest Floquet multiplier is a positive real value when the system is unperturbed. It has been known that the delayed feedback method, including the EDF method, can stabilize only a certain class of periodic orbits with a finite torsion [17]. The period-4 positive current cannot be stabilized at $R \leq 0.8$ because it has a greater degree of instability ($\Lambda_1 \simeq -862, \Omega_1 = 0$) when $K = 0$. The period-4 negative current can be stabilized even at $R = 0$. λ^* of the period-4 orbits ($\tau = 4T = 8\pi/\omega_0$) is numerated as $\lambda^* \simeq -0.0429$ ($R = 0.2$), -0.0244 ($R = 0.4$), -0.0136 ($R = 0.6$), and -0.0059 ($R = 0.8$).

All periodic orbits in Figs. 4, 5, 6, and 7 have common properties. When $K = 0$, their largest Floquet multipliers are real and negative so that the corresponding leading Floquet exponents satisfy $\omega_1 = \pi/\tau$. It means that all UPOs flip their neighborhood within the period τ in the unperturbed system. The variation of each orbit's largest Floquet multiplier depending on the feedback strength K has a common aspect as shown in Fig. 8. We plot the loci of the largest Floquet multiplier of period-2 nega-

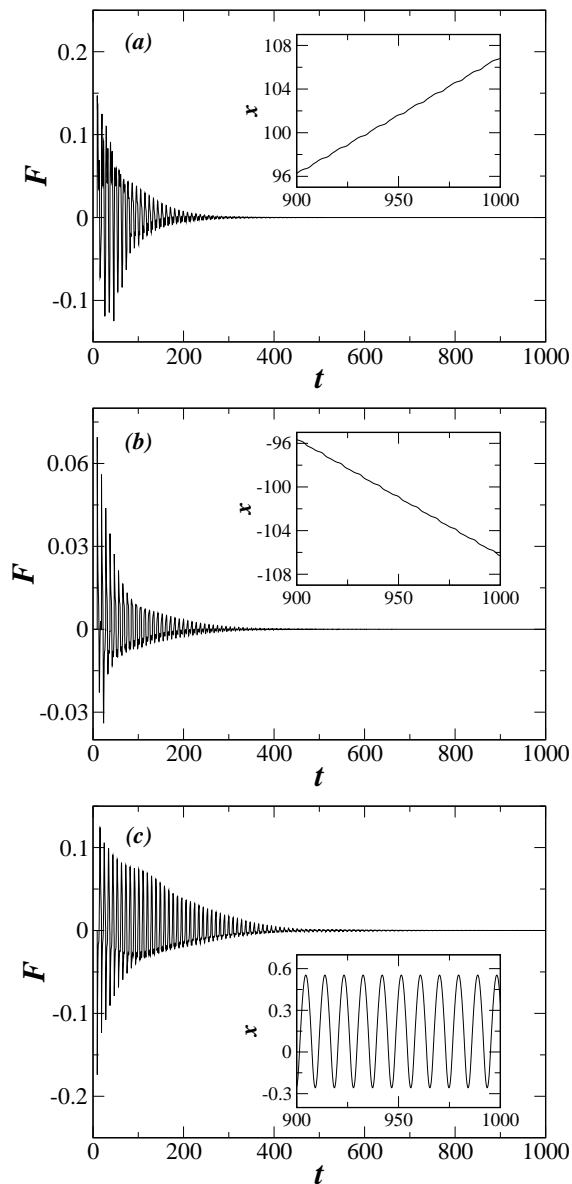


FIG. 9: Stabilized period-1 orbits (insets) and the dynamics of the control signal F at $K = 0.67$, $R = 0.8$, and $\tau = T = 2\pi/\omega_0$; (a) the positive current from the initial condition $(x_0, v_0) = (-0.35, 0.2)$, (b) the negative current from $(0.2, 0.0)$, and (c) the confined current from $(0.0, 0.0)$.

tive orbit at $R = 0.2$ (Fig. 8(a)), and at $R = 0.6$ (Fig. 8(b)). Let us see Fig. 8(a). As K increases, the largest Floquet multiplier moves toward the zero point in remaining a negative real value and crosses the unit circle so that the period-2 negative orbit is stabilized ($\lambda_1 < 0$). With the further increase of K , the largest Floquet multiplier becomes a complex value. It is precisely at this point that the leading Floquet exponent λ_1 has a minimum value (see Fig. 5(b) for the case of $R = 0.2$). Then the pair of complex conjugates move symmetrically and walk out of the unit circle so that the periodic orbit is destabilized. For $K \rightarrow \infty$, the largest Floquet multiplier

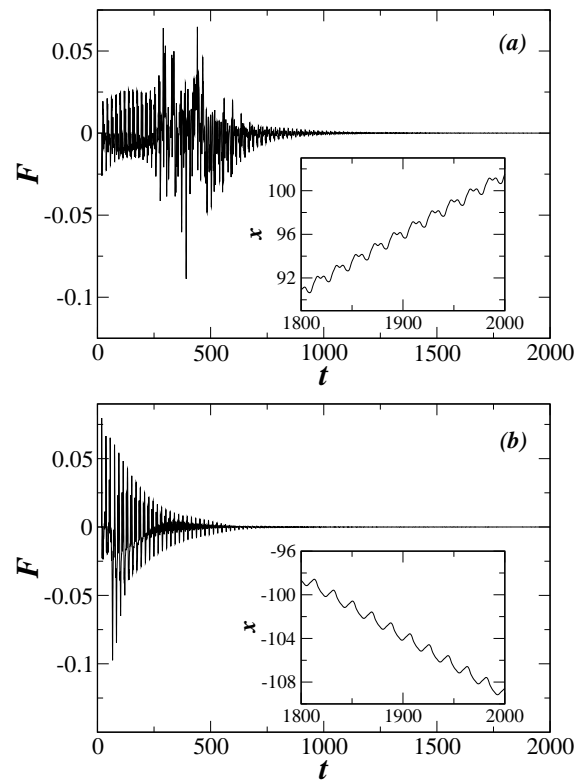


FIG. 10: Stabilized period-2 orbits (insets) and the dynamics of the control signal F at $K = 0.35$, $R = 0.8$, and $\tau = 2T = 4\pi/\omega_0$; (a) the positive current from the initial condition $(x_0, v_0) = (0.0, 0.0)$, and (b) the negative current from $(0.0, 0.1)$.

approaches $(\Lambda_1, \Omega_1) = (1, 0)$ very slowly. In the same manner with Fig. 8(a), the largest Floquet multiplier in Fig. 8(b) (at $R = 0.6$) moves toward the zero point as K increases, until it meets the inner circle of radius R . Then, it jumps to the opposite side of the inner circle and becomes a complex value. In some finite interval of K , the pair of complex conjugates follow a curved line, which is very close to the inner circle. The loci of the largest Floquet multiplier in this interval explain the presence of a flat bottom in Fig. 5(b) for the case of $R = 0.6$. (When the Floquet multiplier locates on the inner circle of radius R , the corresponding Floquet exponent is $\lambda = \ln |\Lambda + i\Omega|/\tau = \ln(R)/\tau = \lambda^*$.) Finally, the pair walk out of the unit circle and approach $(\Lambda_1, \Omega_1) = (1, 0)$.

IV. CONTROL OF TRANSPORT PROPERTIES

With the results of linear stability analysis of periodic orbits, we can obtain a desired transport property of the system (i.e., a regular current with a desired mean velocity) by choosing the control parameters (K, R, τ) where the corresponding UPO is stabilized. For simple and efficient application of the EDF method, it is hoped that each UPO has its own stabilized region of control param-

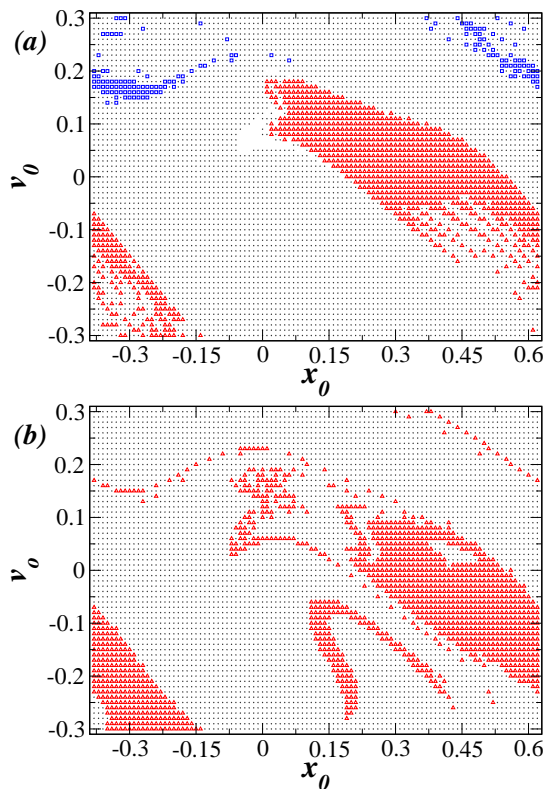


FIG. 11: (Color online) (a) Basins of period-1 orbits; the initial points marked by \square (blue), \triangle (red), and \cdot (black) are the basins of the positive, the negative, and the confined currents, respectively. (b) Basins of period-2 orbits; the initial points marked by \cdot (black) and \triangle (red) are the basins of the positive and the negative currents, respectively.

eters, in which the other UPOs still remain in an unstable state. Some of the UPOs have their own stabilized regions of control parameters. These orbits are the period-1 confined, the period-2 negative, the period-3 positive, and the period-4 negative currents. For the cases of the period-1 positive, the period-1 negative, and the period-2 positive currents, the stabilization of each periodic orbit is rather complex because they do not have their own stabilized regions of control parameters. The stabilized region of the period-1 positive and the negative currents always overlaps with that of the period-1 confined current, and the stabilized region of the period-2 positive current overlaps with that of the period-2 negative current.

Now, we are interested in the multistable phenomenon that more than one UPOs are stabilized at the same control parameters (K, R, τ) . At control parameters, $K = 0.67$, $R = 0.8$, and $\tau = T = 2\pi/\omega_0$, all of period-1 orbits are stabilized. In Fig. 4, each of the leading Floquet exponents of the period-1 orbits at these parameters is marked by a black circle and all of them are less than zero. Also, all of period-2 orbits are stabilized at $K = 0.35$, $R = 0.8$, and $\tau = 2T = 4\pi/\omega_0$. Each of the leading Floquet exponents of the period-2 orbits at these

parameters is marked by a black circle in Fig. 5. In the unperturbed system ($K = 0$), all of the initial conditions evolve into a chaotic current in the same manner. However, the system controlled by the EDF method shows different currents for different initial conditions (x_0, v_0) , at control parameters where the multistable phenomenon is observed.

Before considering the numerical integration for obtaining dynamics of the system controlled by the EDF method, we rewrite the control signal $F(t)$ given in Eq. (5) into a more convenient form

$$\begin{aligned} F(t) &= K((1-R)S(t-\tau) - \dot{x}(t)), \\ S(t) &= \dot{x}(t) + RS(t-\tau), \end{aligned} \quad (13)$$

where $S(t) = \sum_{m=0}^{\infty} R^m \dot{x}(t-m\tau)$ for an equivalent equation with Eq. (5) (see Ref. [24]). In the following numerical integrations, we set $S(t') = 0$ for t' in the interval $[-\tau, 0]$ and initialize $S(t') = \dot{x}(t')/(1-R)$ for t' in the interval $[0, \tau]$. Then, the system is not perturbed ($F = 0$) for t in the interval $[0, \tau]$ and perturbed by the control signal from $t = \tau$. In Fig. 9, we have plotted three stabilized period-1 orbits that evolved from different initial conditions and the dynamics of the control signal F at the same control parameters, $K = 0.67$, $R = 0.8$, and $\tau = T = 2\pi/\omega_0$. For each initial condition, we have integrated Eqs. (4) and (13). In Fig. 10, we have shown two stabilized period-2 orbits that evolved from different initial conditions and the dynamics of the control signal F at $K = 0.35$, $R = 0.8$, and $\tau = 2T = 4\pi/\omega_0$. The multistable phenomenon shows that the EDF method can be utilized for separation of particles in the deterministic inertia ratchet system. Via the EDF method, we can separate particles in the deterministic inertia ratchet system as their initial conditions vary. In Fig. 11, we have investigated the basins of period-1 and period-2 orbits. We have integrated Eqs. (4) and (13) with the initial condition (x_0, v_0) , where x_0 is distributed in one well of the potential, $x_0 \in (-0.38, 0.62)$, and v_0 is confined to the ranges of velocities in the unperturbed system, $v_0 \in (-0.3, 0.3)$. As shown in Fig. 11(a), the basins of the period-1 positive, the negative, and the confined currents are marked by \square (blue), \triangle (red), and \cdot (black), respectively. The basins of the period-2 positive and the negative currents are marked by \cdot (black) and \triangle (red), respectively, in Fig. 11(b).

V. CONCLUSIONS

We have studied the control of transport properties in the deterministic inertia ratchet system via the extended delay feedback method. We have controlled a chaotic current of the unperturbed system to a regular current, which has a desired mean velocity. To obtain the control parameters in which the corresponding unstable periodic orbit is stabilized, we solve the leading Floquet exponent

in the presence of the extended delay feedback. With the results of leading Floquet exponents as a function of control parameters, we have obtained a desired regular transport property of the system. Also, we have observed the multistable phenomenon that more than one unstable periodic orbits are stabilized at the same control parameters and we have shown that the extended delay feedback method can be utilized for separation of particles as a particle's initial condition varies.

Acknowledgments

The authors thank Dr. S. Rim for valuable discussions. This study was supported by the Creative Research Initiatives (Center for Controlling Optical Chaos) of MOST/KOSEF.

-
- [1] P. Reimann, Phys. Rep. **361**, 57 (2002).
 - [2] R. D. Astumian and P. Hänggi, Physics Today **55**, 33 (2002).
 - [3] R. D. Astumian and M. Bier, Phys. Rev. Lett. **72**, 1766 (1994); R. D. Astumian and M. Bier, Biophys. J. **70**, 637 (1996); M. Porto, M. Urbakh, and J. Klafter, Phys. Rev. Lett. **85**, 491 (2000); J. V. Hernández, E. R. Kay, and D. A. Leigh, Science **306**, 1532 (2004).
 - [4] I. Zapata, R. Bartussek, F. Sols, and P. Hänggi, Phys. Rev. Lett. **77**, 2292 (1996); C. C. de Souza Silva, J. V. de Vondel, M. Morelle, and V. V. Moshchalkov, Nature **440**, 651 (2006).
 - [5] P. Reimann, M. Grifoni, and P. Hänggi, Phys. Rev. Lett. **79**, 10 (1997); M. Grifoni, M. S. Ferreira, J. Peguiron, and J. B. Majer, *ibid.* **89**, 146801 (2002).
 - [6] K. H. Lee, Appl. Phys. Lett. **83**, 117 (2003); D. E. Shalóm and H. Pastoriza, Phys. Rev. Lett. **94**, 177001 (2005); M. Beck, E. Goldobin, M. Neuhaus, M. Siegel, R. Kleiner, and D. Kolle, *ibid.* **95**, 090603 (2005); K. H. Lee, J. Korean Phys. Soc. **47**, 288 (2005).
 - [7] J. Rousselet, L. Salome, A. Ajdari, and J. Prost, Nature **370**, 446 (1994).
 - [8] R. Bartussek, P. Reimann, and P. Hänggi, Phys. Rev. Lett. **76**, 1166 (1996); T. E. Dyalynas, K. Lindenberg, and G. P. Tsironis, Phys. Rev. E **56**, 3976 (1997).
 - [9] M. O. Magnasco, Phys. Rev. Lett. **71**, 1477 (1993); I. Derényi and T. Vicsek, *ibid.* **75**, 374 (1995).
 - [10] M. Barbi and M. Salerno, Phys. Rev. E **63**, 066212 (2001).
 - [11] S. Savel'ev, F. Marchesoni, P. Hänggi, and F. Nori, Phys. Rev. E **70**, 066109 (2004).
 - [12] M. Kostur, P. Hänggi, P. Talkner, and J. L. Mateos, Phys. Rev. E **72**, 036210 (2005).
 - [13] W.-S. Son, Y.-J. Park, J.-W. Ryu, D.-U. Hwang, and C.-M. Kim, to be published in J. Korean Phys. Soc.
 - [14] E. Ott, C. Grebogi, and J. A. Yorke, Phys. Rev. Lett. **64**, 1196 (1990).
 - [15] T. Shinbrot, C. Grebogy, E. Ott, and J. A. Yorke, Nature **363**, 411 (1993); *Handbook of Chaos Control*, edited by H. G. Schuster (Wiley-VCH, Weinheim, 1999); S. Boccaletti, C. Grebogi, Y.-C. Lai, H. Mancini, and D. Maza, Phys. Rep. **329**, 103 (2000).
 - [16] K. Pyragas, Phys. Lett. A **170**, 421 (1992).
 - [17] T. Ushio, IEEE Trans. Circuits Syst. I, Fundam. Theory Appl. **43**, 815 (1996); W. Just, T. Bernard, M. Osthmer, E. Reibold, and H. Benner, Phys. Rev. Lett. **78**, 203 (1997); H. Nakajima, Phys. Lett. A **232**, 207 (1997); W. Just, E. Reibold, H. Benner, K. Kacperski, P. Fronczak, and J. A. Holyst, Phys. Lett. A **254**, 158 (1999).
 - [18] J. E. S. Socolar, D. W. Sukow, and D. J. Gauthier, Phys. Rev. E **50**, 3245 (1994).
 - [19] A. Kittel, J. Parisi, and K. Pyragas, Phys. Lett. A **198**, 433 (1995); H. G. Schuster and M. B. Stemmler, Phys. Rev. E **56**, 6410 (1997); K. Pyragas, Phys. Rev. Lett. **86**, 2265 (2001).
 - [20] M. E. Bleich and J. E. S. Socolar, Phys. Lett. A **210**, 87 (1996); W. Just, E. Reibold, K. Kacperski, P. Fronczak, J. A. Holyst, and H. Benner, Phys. Rev. E **61**, 5045 (2000); K. Pyragas, Phys. Rev. E **66**, 026207 (2002).
 - [21] J. L. Mateos, Phys. Rev. Lett. **84**, 258 (2000).
 - [22] W.-S. Son, I. Kim, Y.-J. Park, and C.-M. Kim, Phys. Rev. E **68**, 067201 (2003).
 - [23] M. Barbi and M. Salerno, Phys. Rev. E **62**, 1988 (2000).
 - [24] K. Pyragas, Phys. Lett. A **206**, 323 (1995).